

Measurement of longitudinal and transverse cross sections in the ${}^3\text{He}(e, e' \pi^+) {}^3\text{H}$ reaction at $W=1.6$ GeV

D. Gaskell,^{10,1,*} A. Ahmidouch,⁸ P. Ambrozewicz,¹³ H. Anklin,^{3,14} J. Arrington,¹ K. Assamagan,⁴ S. Avery,⁴ K. Bailey,¹ O. K. Baker,^{4,14} S. Beedoe,⁸ B. Beise,⁶ H. Breuer,⁶ D. S. Brown,⁶ R. Carlini,¹⁴ J. Cha,⁴ N. Chant,⁶ A. Cowley,⁶ S. Danagoulian,^{8,14} D. De Schepper,¹ J. Dunne,¹⁴ D. Dutta,⁹ R. Ent,¹⁴ L. Gan,⁴ A. Gasparian,⁴ D. F. Geesaman,¹ R. Gilman,^{12,14} C. Glashauser,¹² P. Gueye,⁴ M. Harvey,⁴ O. Hashimoto,¹⁵ W. Hinton,⁴ G. Hofman,² C. Jackson,⁸ H. E. Jackson,¹ C. Keppel,^{4,14} E. Kinney,² D. Koltenuk,¹¹ A. Lung,¹⁴ D. Mack,¹⁴ D. McKee,⁷ J. Mitchell,¹⁴ H. Mkrtchyan,¹⁸ B. Mueller,¹ G. Niculescu,⁴ I. Niculescu,⁴ T. G. O'Neill,¹ V. Papavassiliou,^{7,14} D. Potterveld,¹ J. Reinhold,¹ P. Roos,⁶ R. Sawafta,⁸ R. Segel,⁹ S. Stepanyan,¹⁸ V. Tadevosyan,¹⁸ T. Takahashi,¹⁵ L. Tang,^{4,14} B. Terburg,⁵ D. Van Westrum,² J. Volmer,^{17,†} T. P. Welch,¹⁰ S. Wood,¹⁴ L. Yuan,⁴ B. Zeidman,¹ and B. Zihlmann^{14,16}

¹Argonne National Laboratory, Argonne, Illinois 60439

²University of Colorado, Boulder, Colorado 76543

³Florida International University, Miami, Florida 33119

⁴Hampton University, Hampton, Virginia 23668

⁵University of Illinois, Champaign, Illinois 61801

⁶University of Maryland, College Park, Maryland 20742

⁷New Mexico State University, Las Cruces, New Mexico 88003

⁸North Carolina A & T State University, Greensboro, North Carolina 27411

⁹Northwestern University, Evanston, Illinois 60201

¹⁰Oregon State University, Corvallis, Oregon 97331

¹¹University of Pennsylvania, Philadelphia, Pennsylvania 19104

¹²Rutgers University, Piscataway, New Jersey 08855

¹³Temple University, Philadelphia, Pennsylvania 19122

¹⁴Thomas Jefferson National Accelerator Facility, Newport News, Virginia 23606

¹⁵Tohoku University, Sendai 982, Japan

¹⁶University of Virginia, Charlottesville, Virginia 22901

¹⁷Vrije Universiteit, NL-1081 HV Amsterdam, The Netherlands

¹⁸Yerevan Physics Institute, 375036 Yerevan, Armenia

(Received 9 October 2001; published 21 December 2001)

The coherent ${}^3\text{He}(e, e' \pi^+) {}^3\text{H}$ reaction was measured at $Q^2=0.4$ (GeV/c)² and $W=1.6$ GeV for two values of the virtual photon polarization, ϵ , allowing the separation of longitudinal and transverse cross sections. The results from the coherent process on ${}^3\text{He}$ were compared to $\text{H}(e, e' \pi^+)n$ data taken at the same kinematics. This marks the first direct comparison of these processes. At these kinematics ($p_\pi=1.1$ GeV/c), pion rescattering from the spectator nucleons in the ${}^3\text{He}(e, e' \pi^+) {}^3\text{H}$ process is expected to be small, simplifying the comparison to π^+ production from the free proton.

DOI: 10.1103/PhysRevC.65.011001

PACS number(s): 25.30.Rw, 25.30.Dh, 13.60.Le, 25.10.+s

The ${}^3\text{He}(e, e' \pi^+) {}^3\text{H}$ process holds much theoretical interest in that the mass-3 system is calculable using “exact” Fadeev-type wave functions and hence serves as a good test of our understanding of nuclei. In addition, comparison to the fundamental $\text{H}(e, e' \pi^+)n$ process may shed some light on medium modifications to the pion electroproduction process. In general, one expects the ${}^3\text{He}(e, e' \pi^+) {}^3\text{H}$ cross section to be suppressed by a factor roughly proportional to the square of the ${}^3\text{He}$ form factor. Significant deviations from this behavior may signal changes to the pion electroproduction process in the nucleus. In Refs. [1,2], the comparison of ${}^3\text{He}(e, e' \pi^+) {}^3\text{H}$ separated cross sections (σ_L and σ_T in Ref. [2] and σ_L , σ_T , and σ_{LT} in Ref. [1]) to a distorted-wave impulse approximation (DWIA) calculation indicates that the

fundamental pion electroproduction process is indeed modified in the nuclear medium and that these modifications can be explained in terms of modifications to the pion-pole propagator and the width of the Δ resonance. The pion-pole propagator modification is particularly interesting in that such a mechanism has been used to predict the enhancement of nuclear longitudinal response functions which in turn suggests the presence of “extra” pions in the nucleus coming from pion exchange between nucleons [3].

While the results in Refs. [1,2] are interesting, they are limited by the fact that the ${}^3\text{He}(e, e' \pi^+) {}^3\text{H}$ data are compared to a DWIA calculation. The fundamental $\text{H}(e, e' \pi^+)n$ cross section model (the Unitary Isobar MAID Model of Ref. [4]) used as the input to the DWIA calculation has been shown to be consistent with most existing photo- and electroproduction data. However, the majority of the electroproduction data give unseparated cross sections (i.e., $\sigma = \sigma_T + \epsilon\sigma_L$) and the validity of the MAID σ_L and σ_T decompo-

*Present address: University of Colorado, Boulder, CO 80309.

†Present address: DESY Zeuthen, D-15738 Zeuthen, Germany.

TABLE I. Spectrometer settings for the ${}^3\text{He}(e, e' \pi^+) {}^3\text{H}$ [and $\text{H}(e, e' \pi^+) n$] subset of the E91003 experiment presented in this work.

ϵ	E_{beam} (GeV)	P_{HMS} (GeV/c)	θ_{HMS}	P_{SOS} (GeV/c)	θ_{SOS}
0.490	1.65	0.54	39.3°	1.00	15.5°
0.894	3.25	2.14	13.8°	1.00	23.5°

sition cannot be verified at the kinematics of Refs. [1,2]. Real photon data on both ${}^3\text{He}(\gamma, \pi^+) {}^3\text{H}$ and $\text{H}(\gamma, \pi^+) n$ exist [5], but unfortunately this is only sensitive to the transverse piece of the cross section and hence does not shed light on the pion pole term, which manifests itself in the longitudinal channel. A further complication with the existing photo- and electro-production data is that in both cases the final pion momentum is near the Δ resonance, and hence the effect from pion rescattering on the spectator nucleons in ${}^3\text{He}$ is considerable.

The ${}^3\text{He}(e, e' \pi^+) {}^3\text{H}$ data presented here benefit from the fact that the final pion momentum is significantly larger ($p_\pi = 1.1$ GeV/c) than that in previous measurements. At this momentum, the pion-nucleon center-of-mass energy, W , is still in the resonance region [just above the $S_{11}(1535)$], but well away from the prominent $\Delta(1232)$ leading to much smaller pion rescattering effects. Furthermore, this work gives the first direct comparison of the separated longitudinal and transverse cross sections from ${}^3\text{He}(e, e' \pi^+) {}^3\text{H}$ to those from $\text{H}(e, e' \pi^+) n$.

The results in this work come from data obtained during Jefferson Lab experiment E91003—a study of charged pion electroproduction from H, ${}^2\text{H}$, and ${}^3\text{He}$ that was carried out in experimental Hall C. This subset of the E91003 data was obtained using beam energies of 1.645 GeV and 3.245 GeV and made use of high-density cryogenic H and ${}^3\text{He}$ targets. Electrons were detected in the High Momentum Spectrometer (HMS) and pions in the Short Orbit Spectrometer (SOS). In this work we present the results from the coherent channel, ${}^3\text{He}(e, e' \pi^+) {}^3\text{H}$, and compare them to those from $\text{H}(e, e' \pi^+) n$. Results from the ${}^3\text{He}(e, e' \pi^\pm)$ continuum channels ($Dn + pnn$ final states for π^+ and ppp final state for π^-) have been presented elsewhere [6]. The ${}^3\text{He}(e, e' \pi^+) {}^3\text{H}$ process was measured in parallel kinematics (the pion direction along the virtual photon momentum, \mathbf{q}) at $Q^2 = 0.4$ (GeV/c) 2 and $W = 1.6$ GeV (for the free nucleon) at two values of the virtual photon polarization parameter, ϵ (0.49 and 0.89). At these kinematics the final pion momentum was $p_\pi = 1.1$ GeV/c. The experimental kinematics are summarized in Table I. The H and ${}^3\text{He}$ data were taken with the same experimental configuration.

Electrons in the HMS were selected using a gas Čerenkov containing C_4F_{10} at 0.42 atmospheres. Pions in the SOS were identified using time-of-flight information from two pairs of scintillating hodoscope arrays to reject protons. Backgrounds from random coincidences and the aluminum walls of the cryogenic targets were subtracted in the charge-normalized yields.

The ${}^3\text{H}$ final state in the ${}^3\text{He}$ data was selected via cuts on M_x , the reconstructed missing mass of the recoiling

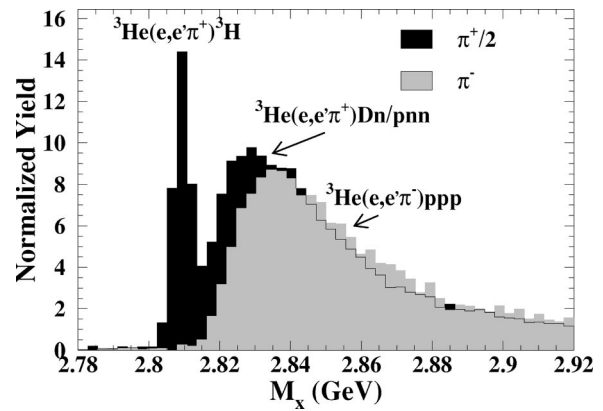


FIG. 1. Missing mass distributions for π^+ and π^- production from ${}^3\text{He}$ at the $\epsilon = 0.89$ kinematics. Since π^+ production can proceed via either of the two protons in ${}^3\text{He}$ and π^- only from the single neutron, the π^+ data have been divided by 2 for comparison with the π^- data. The coherent ${}^3\text{H}$ final state is clearly distinguishable from the $Dn + pnn$ continuum states.

system, $M_x^2 = (q + P_{\text{He}} - p_\pi)^2$. A sample missing mass spectrum for π^+ and π^- production from ${}^3\text{He}$ is shown in Fig. 1. The ${}^3\text{H}$ final state is clearly visible in the π^+ spectrum.

The pion electroproduction cross section can be written

$$\frac{d\sigma}{d\Omega_e dE_e d\Omega_\pi} = \Gamma \frac{d\sigma}{d\Omega_\pi}, \quad (1)$$

where $d\sigma/d\Omega_\pi$ is the virtual photon cross section (evaluated in the laboratory frame), and Γ is the virtual photon flux factor given by

$$\Gamma = \frac{\alpha}{2\pi^2} \frac{E'_e}{E_e} \frac{1}{Q^2} \frac{1}{1-\epsilon} \frac{W^2 - M^2}{2M}. \quad (2)$$

Since we are in part interested in the comparison between the H and ${}^3\text{He}$ cross sections, we take M in Eq. (2) (as well as in the calculation of W) to be the nucleon mass for both targets so that equal lab cross sections result in equal virtual photon cross sections regardless of target mass.

The twofold virtual photon cross section can be written

$$\begin{aligned} \frac{d\sigma}{d\Omega_\pi} &= \frac{d\sigma_T}{d\Omega_\pi} + \epsilon \frac{d\sigma_L}{d\Omega_\pi} + \epsilon \frac{d\sigma_{TT}}{d\Omega_\pi} \cos 2\phi_{pq} \\ &+ \sqrt{2\epsilon(1+\epsilon)} \frac{d\sigma_{LT}}{d\Omega_\pi} \cos \phi_{pq}, \end{aligned} \quad (3)$$

where ϵ describes the longitudinal polarization of the virtual photon. In the parallel kinematics of this experiment, the interference terms (σ_{LT} and σ_{TT}) are small, and for complete ϕ_{pq} coverage integrate to zero.

The experimental cross sections were extracted using a Monte Carlo of the experiment that included detailed descriptions of the spectrometer magnetic elements and apertures, decay of the pions in flight, multiple scattering, ionization energy loss, and radiative effects. The efficacy of the Monte Carlo was verified using elastic $\text{H}(e, e' p)$ and $\text{H}(e, e' n)$ data. The Monte Carlo yield, modeled using a pa-

rametrization of the elastic cross section [7], was found to agree with the experimental elastic yield to within 3.5% (the total uncertainty on the elastic data). In modeling the pion electroproduction data, the Monte Carlo used the MAID [4] model of charged pion electroproduction from nucleons to account for variations of the cross section across the experimental acceptance. For the ${}^3\text{He}(e, e' \pi^+) {}^3\text{H}$ process, the kinematic variation of the cross section was assumed to be the same as for π^+ production from the free proton.

Although the MAID model provided a good starting point, an iterative procedure was used to reduce the dependence of the extracted experimental cross sections on the pion electroproduction model. In this procedure, the contribution from the $Dn + pnn$ continuum states (to be discussed below) was fit once and its relative contribution to the yield for $M_x < 2.815$ GeV fixed. Then, the simulation was compared to the measured yield, and a correction function was fit for a complete set of kinematic variables (Q^2 , ν , θ_{pq} , and ϕ_{pq}). The final iterated model was then the original MAID model multiplied by the correction function. Further details of the analysis can be found in Ref. [12].

Since the experimental resolution was not sufficient to completely separate the coherent ${}^3\text{H}$ final state from the continuum $Dn + pnn$ states, it was necessary to model the latter and include them in the simulation. The $Dn + pnn$ final states were modeled in the Monte Carlo in a quasifree approximation that convolved the $\gamma^* - N$ cross section with a realistic nucleon momentum distribution [8] (calculated using the techniques described in Ref. [9]). A missing energy distribution fit from ${}^3\text{He}(e, e' p)$ data [10] was also used which helped model the Dn strength relative to the pn strength. Effects from nucleon-nucleon final state interactions were included via a simple Jost function prescription [11].

In practice, the ${}^3\text{H}$ and $Dn + pnn$ final states were modeled separately, and their relative strengths determined by fitting the combined missing mass spectrum to the data up to $M_x = 2.84$ GeV. An example of such a fit is shown in Fig. 2 for the $\epsilon = 0.49$ data (the qualitative features of such a fit to the $\epsilon = 0.89$ data are very similar).

The result of this fit was used to determine the $Dn + pnn$ contribution to the yield for $M_x < 2.815$ GeV. Note that the data are well described, except for the region $2.815 \text{ GeV} < M_x < 2.82$ GeV, where the Monte Carlo significantly overpredicts the experimental yield. In this region, the shape of the $Dn + pnn$ missing mass distribution is driven by nucleon-nucleon final state interactions and the Jost function corrections are large. A more sophisticated treatment of these effects would likely improve the agreement between the data and Monte Carlo in these bins, but the contribution to the uncertainty in the ${}^3\text{H}$ cross section due to the modeling of the nucleon-nucleon final state interactions is not large. The contribution to the experimental yield for $M_x < 2.185$ GeV from the $Dn + pnn$ final states was estimated to be 4%(8%) at low(high) ϵ , where the variation of the contribution comes mostly from the difference in resolution between the low and high ϵ settings. The uncertainty in the ${}^3\text{H}$ yield due to this correction was estimated by modifying the strength of the nucleon-nucleon final state interac-

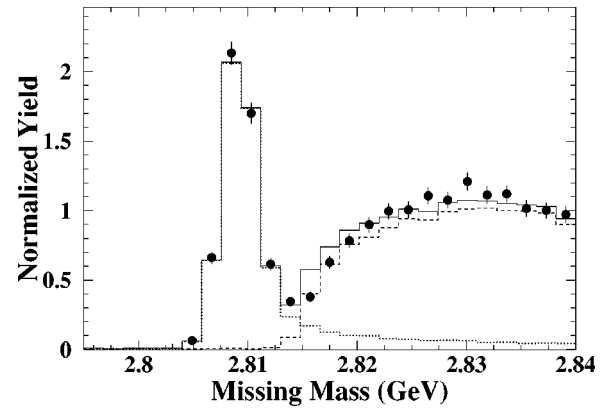


FIG. 2. Data and Monte Carlo missing mass distributions for ${}^3\text{He}(e, e' \pi^+)$ at $\epsilon = 0.49$. The solid curve is the total simulation while the dotted and dashed curves are the simulation of the ${}^3\text{H}$ and $Dn + pnn$ final states, respectively. The latter was used to estimate the continuum background to the ${}^3\text{H}$ final state for $M_x < 2.815$ GeV.

tions in the simulation and was determined to be 3% correlated (1% uncorrelated) between ϵ settings. An additional 1% correlated (0.75–1% uncorrelated) uncertainty was assigned due to slight differences in the missing mass peak widths between the data and Monte Carlo.

The statistical precision on the unseparated cross sections was typically 0.8% for the H data and 1.9–2.5% for the ${}^3\text{H}$ data. Correlated systematic uncertainties were 5.5–6.3%, the largest sources coming from pion absorption in the targets and spectrometers (3.5%), spectrometer acceptance (2%), radiative corrections (2.2%), and pion decay in-flight (2%). The correlated uncertainties propagate directly into the separated cross sections and cancel in the separated and unseparated ratios. The uncorrelated systematic uncertainties contribute randomly at each ϵ and contribute to the target ratios. The uncorrelated systematic uncertainties were 1.7–2.3%. Significant sources were the iteration and cross section extraction procedure (0.8%), spectrometer acceptance (0.5%), radiative corrections (0.5%), pion decay (0.5%), and uncertainties in kinematic quantities (0.1–1.4%). Additionally, the

TABLE II. Unseparated and separated laboratory cross sections for $\text{H}(e, e' \pi^+)n$ and ${}^3\text{He}(e, e' \pi^+) {}^3\text{H}$ reactions at $W = 1.6$ GeV, $Q^2 = 0.4$ (GeV/c) 2 , and $\theta_{pq} = 1.72^\circ$. Uncertainties are statistical and systematic. A common value of the virtual photon flux Γ has been used in extracting the virtual photon cross sections to facilitate comparisons between the targets.

	$d\sigma/d\Omega_\pi$ ($\mu\text{b}/\text{sr}$)	
	${}^3\text{H}$	H
Unseparated cross sections		
$\epsilon = 0.490$	$14.89 \pm 0.36 \pm 1.00$	$44.23 \pm 0.36 \pm 2.52$
$\epsilon = 0.894$	$21.80 \pm 0.40 \pm 1.50$	$58.18 \pm 0.44 \pm 3.42$
Separated cross sections		
σ_L	$17.12 \pm 1.36 \pm 2.38$	$34.57 \pm 1.41 \pm 4.38$
σ_T	$6.50 \pm 0.95 \pm 1.45$	$27.29 \pm 0.96 \pm 2.89$

TABLE III. Unseparated and separated cross section ratios for $H(e, e' \pi^+)n$ and ${}^3\text{He}(e, e' \pi^+){}^3\text{H}$ reactions. Uncertainties are statistical and systematic.

	$R = \sigma({}^3\text{H})/\sigma(\text{H})$
Unseparated ratios	
$\epsilon = 0.490$	$0.337 \pm 0.009 \pm 0.012$
$\epsilon = 0.894$	$0.375 \pm 0.008 \pm 0.015$
Separated ratios	
σ_L	$0.496 \pm 0.044 \pm 0.072$
σ_T	$0.238 \pm 0.036 \pm 0.042$

integrated beam current was assigned a 1% correlated and 0.5% uncorrelated systematic uncertainty. The ${}^3\text{H}$ results also included uncertainties due to the $Dn + pnn$ background modeling and missing mass peak width differences discussed above.

The unseparated and separated H and ${}^3\text{H}$ cross sections are given in Table II. These cross sections are given in the laboratory frame at $Q^2 = 0.4$ (GeV/c)² and $\theta_{pq} = 1.72^\circ$. The cross section ratios are shown in Table III. It is clear that both the separated and unseparated cross sections from the coherent process are, as expected, suppressed relative to the free nucleon cross section. Note that the ratios in Table III are not normalized to the number of contributing nucleons (i.e., the ${}^3\text{He}$ results are not divided by 2)—this is in contrast to our earlier results presented in Ref. [6].

A calculation comparing coherent π^+ production from ${}^3\text{He}$ to that from H for similar values of the momentum transfer to the nucleus was performed in Ref. [13]. In this work, the ratio of the ${}^3\text{He}$ to H cross sections was dominated by the square of the ${}^3\text{He}$ form factor, $F(k)$, where k is the momentum transfer to the nucleus. At small k , this can be represented in a Gaussian form,

$$F^2(k) = \exp(-k^2/18a), \quad (4)$$

where we take $a = 0.064$ fm⁻² as in Ref. [13]. In our kinematics, $k = 0.19$ GeV/c so $F^2(k) = 0.447$. Note that in the impulse approximation, only one proton in ${}^3\text{He}$ contributes to the cross section due to the Pauli exclusion principle. The target ratio is further suppressed by the fact that the final pion momenta in the ${}^3\text{He}(e, e' \pi^+){}^3\text{H}$ and the $H(e, e' \pi^+)n$ processes are not the same and hence we must account for the difference in the density of final states. This factor yields 0.95, so that the net suppression is ≈ 0.42 . We do not expect pion rescattering to significantly impact our ${}^3\text{H}$ cross sections. In a simple factorization approximation, the calculated effect of rescattering depends only on the final pion momen-

tum, p_π , and is less than 3% [14]. Note that the calculations in Ref. [13] are much more complete and include further effects such as the range of propagation of the nucleon and resonance poles and spin-isospin correlations. The calculated suppression we present here is intended only to give a rough sense of the anticipated effect. Nonetheless, we see from Table III that the unseparated ratios are not too dissimilar from our simple estimate. This is also true for the separated ratios, except we see in this case that the transverse channel is suppressed much more than the longitudinal. A similar effect was seen in Refs. [1,2] where the longitudinal (transverse) ${}^3\text{H}$ cross section was significantly larger (smaller) than that estimated using a DWIA calculation. Good agreement between the data of Refs. [1,2] and their DWIA calculation was achieved only after introducing medium modifications. In particular, a modification of the pion propagator in the pole process eliminated the discrepancy seen in the longitudinal channel, while a modification to the in-medium Δ width was used to explain part of the missing strength in the transverse channel. It would be interesting to see if detailed calculations that include these nuclear effects on the pion propagator and resonance widths explain the difference between the longitudinal and transverse separated ratios presented in this work. Note that while one does not expect the Δ resonance to play a prominent role at our kinematics ($W = 1.6$ GeV) it is possible that medium effects in other resonances [i.e., the nearby $S_{11}(1535)$] may be important.

In summary, this work presents unseparated and separated cross sections for the coherent ${}^3\text{He}(e, e' \pi^+){}^3\text{H}$ process. This experiment improves upon previous ${}^3\text{H}$ experiments by measuring the cross section for a large final pion momentum such that rescattering effects should be small. Furthermore, this marks the first direct comparison of separated longitudinal and transverse ${}^3\text{He}(e, e' \pi^+){}^3\text{H}$ cross sections to those from the free proton. Our results are consistent with the expectation that the suppression of the ${}^3\text{He}$ cross section relative to H is dominated by the ${}^3\text{He}$ form factor, indicating that the gross behavior of the reaction is understood and is an excellent candidate for more detailed theoretical calculation. Indeed, the fact that the transverse strength is significantly more suppressed than the longitudinal indicates that such calculations are necessary to establish whether the observed effect is a result of known processes or is a result of modifications to the pion electroproduction process in the nuclear medium. In particular, it would be interesting to see if our results require medium modifications to the pion propagator, resonance widths, or both.

We thank Lothar Tiator for providing the FORTRAN code for the MAID model. This research was supported by the U.S. National Science Foundation and the U.S. Department of Energy.

[1] M. Kohl *et al.*, nucl-ex/0104004.

[2] K.I. Blomqvist *et al.*, Nucl. Phys. **A626**, 871 (1997).

[3] M. Ericson and A.W. Thomas, Phys. Lett. **128B**, 112 (1983).

[4] D. Drechsel, O. Hanstein, S.S. Kamalov, and L. Tiator, Nucl. Phys. **A645**, 145 (1999); <http://www.kph.uni-mainz.de/MAID>

[5] N. d'Hose *et al.*, Nucl. Phys. **A554**, 679 (1993).

[6] D. Gaskell *et al.*, Phys. Rev. Lett. **87**, 202301 (2001).

[7] P.E. Bosted, Phys. Rev. C **51**, 409 (1995).

[8] R.B. Wiringa (private communication).

[9] J.L. Forest, V.R. Pandharipande, S.C. Pieper, R.B. Wiringa, R.

- Schiavilla, and A. Arriaga, Phys. Rev. C **54**, 646 (1996).
- [10] E. Jans *et al.*, Nucl. Phys. **A475**, 687 (1987).
- [11] J. Gillespie, *Final State Interactions* (Holden-Day, San Francisco, 1964).
- [12] D. Gaskell, Ph.D. thesis, Oregon State University, 2001.
- [13] R.J. Loucks and V.R. Pandharipande, Phys. Rev. C **54**, 32 (1996).
- [14] T.-S. H. Lee (private communication).